Neurovascular reactivity increases across development in the visual and frontal pole networks as revealed by a breath-holding task: a longitudinal fMRI study

Donna Y. Chen[a,b], Xin Di[a], Bharat Biswal[a]

[a] Department of Biomedical Engineering, New Jersey Institute of Technology, Newark, NJ, US

[b] Rutgers Biomedical and Health Sciences, Rutgers School of Graduate Studies, Newark, NJ, US

Correspondence

Bharat Biswal, Ph.D., 607 Fenster Hall, University Heights, Newark, NJ, 07102, US

E-mail: bharat.biswal@njit.edu

Abstract

Functional magnetic resonance imaging (fMRI) has been widely used to understand the neurodevelopmental changes that occur in cognition and behavior across childhood. The blood-oxygen-level-dependent (BOLD) signal obtained from fMRI is understood to be comprised of both neuronal and vascular information. However, it is unclear whether the vascular response is altered across age in studies investigating development in children. Since breath-hold activation is an important aspect to understand the neurovascular response in fMRI studies, it can be used to account for developmental differences in vascular response. This study examines how the vascular response changes over age in a longitudinal children's breath-hold dataset from the Nathan Kline Institute (NKI) Rockland Sample (ages 6 to 18 years old at enrollment). A principal component analysis (PCA) approach was applied to derive brain activation from breath-hold data. To model both the longitudinal and cross-sectional effects of age on breath-hold activation, we used mixed effects modeling with the following terms: linear, quadratic, logarithmic, and quadratic-logarithmic, to find the best-fitting model. We observed increased breath-hold activation in the frontal pole, medial visual, and lateral visual networks across age, in which linear and logarithmic mixed effects models provided the best fit with the lowest Akaike Information Criterion (AIC) scores. This shows that the vascular response increases across development in a brain network-specific manner and may also be nonlinear depending on the brain network. Therefore, fMRI studies investigating the developmental period should account for vascular changes which occur with age.

Key words: fMRI, longitudinal, children, breath-hold, neurovascular reactivity, developmental studies

1. Introduction

The developmental period is a critical time when distinct brain regions undergo rapid growth. With advancements in functional magnetic resonance imaging (fMRI) equipment and analytic methods, we have a better understanding of the developing brain (Davidson et al., 2003; Van Horn and Pelphrey, 2015). fMRI studies have shown differences in brain organization between children and adults, with children having a more localized brain network structure and adults having a more segregated network structure (Fair et al., 2009). Additionally, fMRI studies have revealed developmental changes in cognitive control, such as inhibition response and working memory (Luna et al., 2010), changes in emotional processing in adolescence (Somerville et al., 2010), and altered brain connectivity patterns in children with neurodevelopmental disorders such as autism spectrum disorder (Uddin et al., 2013).

The blood-oxygen-level-dependent (BOLD) fMRI signal is an indirect measure of neuronal activity and is based on the theory of neurovascular coupling, in which an increase in neuronal activity is followed by an increase in blood flow to the particular brain region of activation (Iadecola, 2017). Age-related disruptions in neurovascular coupling have been observed (Abdelkarim et al., 2019; Galiano et al., 2020; Tsvetanov et al., 2015; West et al., 2019) and may be due to an increase in inflammatory signaling that disrupts vasomotor activity (Zimmerman et al., 2021). Furthermore, decreased vascular reactivity in older populations influences the BOLD fMRI signal and may be a confounding factor in studies investigating aging (Kannurpatti et al., 2014). This is important to consider in age-related fMRI studies since differences observed may be mediated by vascular changes rather than neuronal changes. However, little is yet known about the neuronal and vascular contributions of the BOLD signal during childhood. The brain's hemodynamic response is faster in children than that of adults,

since the blood vessel walls tend to stiffen with age, along with changes that occur in the heart rate and respiratory rate which are faster in children (Thomason et al., 2005). Church and colleagues suggest that the developmental differences observed in fMRI studies are not vascular, since the percent BOLD signal change peaks were different among different tasks (Church et al., 2010). However, Schmithorst and colleagues analyzed the ratio of BOLD signal to relative cerebral blood flow (CBF) changes and found increased neurovascular coupling in the middle temporal gyri and the left inferior frontal gyrus with age in children aged 5-18 years (Schmithorst et al., 2015). This supports that the BOLD signal changes may not be driven primarily by neuronal changes, but rather a strong vascular component that influences the changes seen in developmental fMRI studies. Therefore, the vascular properties of the brain contribute to the fMRI signal and need to be further investigated as they may act as a confound.

In order to study the neurovascular properties of the brain with fMRI, the breath-holding task can be used since it focuses more on the vascular contribution of the BOLD signal rather than the neuronal aspect. During the breath-holding task, participants are commonly asked to perform a block-design experiment consisting of blocks of breath-holding ranging from 15-20s, interleaved with blocks of normal-paced breathing ranging from 15-30s (Kastrup et al., 1999b; Kwong et al., 1995; Stillman et al., 1995). The breath-hold response yields an increase in the BOLD fMRI signal, as the demand for oxygen increases following the hypercapnic state during the breath-hold period. This allows researchers to assess the neurovascular response to a vasoactive stimulus, such as increased carbon dioxide levels. As one holds their breath, there is a build-up of carbon dioxide and decrease in pH levels, which leads to the vasodilation of blood vessels that occurs globally in the brain (Bright et al., 2011; Kety and Schmidt, 1948). Other methods used to study the vascular contribution of the BOLD signal are more involved, such as

the intake of acetazolamide or the controlled inhalation of different levels of carbon dioxide gas, which may not be comfortable for participants (Bright et al., 2009; Bruhn et al., 1994; Mukherjee et al., 2005).

Thomason and colleagues reported lower BOLD fMRI signal to noise ratio (SNR) in children compared to that of adults during the performance of a breath-hold task and found a reduced volume of activation in children (Thomason et al., 2005). They also found a heterogeneous vascular response pattern across the brain, which was similar between children and adults. This shows that the BOLD fMRI signal differences reported between groups may not be reflective of differences in neuronal activity but rather reflects the differences in vascular response between groups. However, a limitation of the study includes its cross-sectional design in which comparisons were made between two groups: children (7 to 12 years) and young adults (18 to 29 years). The effect of age on vascular activity may not necessarily be linear but rather have complex trajectories. Therefore, investigating age in one group containing a range of ages may be preferred over comparing results between distinct groups. Furthermore, developmental changes to the BOLD hemodynamic response function (HRF) have been shown in a study comparing neonates to adults, in which neonates had a lower HRF positive peak and longer time-to-peak duration than adults in response to a somatosensory stimulus (Arichi et al., 2012). Additionally, in a study investigating children with epilepsy, significantly longer peak times of the HRF was found in children aged 0 to 2 years old; however, no differences in the HRF were observed between older children and adults with epilepsy (Jacobs et al., 2008). It is not yet clear how the neurovascular reactivity pattern changes across development.

The goal of the current study is to investigate the breath-hold response in children across different ages of development ranging from 6-20 years, using a longitudinal fMRI dataset from

the Nathan Kline Institute (NKI) (Tobe et al., 2022). This dataset includes both longitudinal and cross-sectional data, which allows us to better understand within-subject and between-subject developmental trajectories, respectively. Here, we investigate the neurovascular reactivity changes across development by quantifying the breath-hold response in multiple spatial locations. We fit different types of developmental trajectories to the breath-hold response, including linear, quadratic, logarithmic, and quadratic-log functions and implement a mixed-effects modeling approach to account for the multiple timepoints of data. We hypothesize that the neurovascular response due to breath-hold follows a logarithmic trend in children, in which there is an initial increase in activation followed by a plateau as the microvasculature reaches maturity.

2. Materials and Methods

2.1. Dataset

The Nathan Kline Institute Rockland Sample (NKI-RS) dataset is a community-ascertained collection of multimodal MRI, cognitive, behavioral, and phenotypic data across the lifespan (https://data.rocklandsample.rfmh.org/). For this study, we focused on the NKI-RS Longitudinal Discovery of Brain Development Trajectories sub-study (N=369) (Tobe et al., 2022), which implements a longitudinal design to study connectome development in children. The age at enrollment ranged from 6 to 17 years and the oldest age at completion of the studies is 20 years. We were primarily interested in the fMRI data acquired during the breath-hold paradigm for all healthy subjects, to study vascular activity in the brain due to a vasoactive stimulus. The healthy control (HC) group was defined as having no diagnosis or condition on Axis I of the Diagnostic and Statistical Manual of Mental Disorders (DSM-IV) (Bell, 1994).

For the breath-holding paradigm, there were a total of 7 blocks of breath-holding each lasting 18 seconds, interleaved with 18 second blocks of self-paced breathing. During breath-holding, the participants were shown a circle on a computer screen of decreasing size indicating the duration of breath-holding left. Since this was a longitudinal study, three timepoints were collected from each participant: baseline (BAS1), first follow-up (FLU1), and second follow-up (FLU2). The follow-up sessions were spaced either 12 months or 15 months apart. Some participants enrolled in the 0/12/24 month track while others enrolled in the 0/15/30 month track. We aggregated the subjects on the two tracks together to maximize the number of subjects to be analyzed. Not all participants completed the scans for all three timepoints; however, we included participants who did not complete all three scan timepoints since a mixed effects modeling approach was applied, which is robust to missing data. The NKI study included participants based on the following criteria: 1) ages 6 to 20.5 years (ages 6 to17.9 years at enrollment), 2) children who have the capacity to understand and provide informed consent, 3) children aged 6-17.9 years who can sign assent and parent/guardian who can sign informed consent, 4) fluent in English, and 5) proof of residency in Rockland County, Orange County, Westchester County, NY, or Bergen County, NJ (Tobe et al., 2022).

There was a total of 90 HC subjects who participated in the 18s breath-hold paradigm during the BAS1 session, 82 HC subjects during the FLU1 session, and 60 HC subjects during the FLU2 session. There was a total of 49 HC subjects who completed both BAS1 and FLU1 session, and a total of 22 HC subjects who completed all three sessions (BAS1, FLU1, and FLU2). However, after motion correction, the total data are as follows: 60 BAS1, 55 FLU1, and 40 FLU2 subjects (see preprocessing section for further details on motion correction).

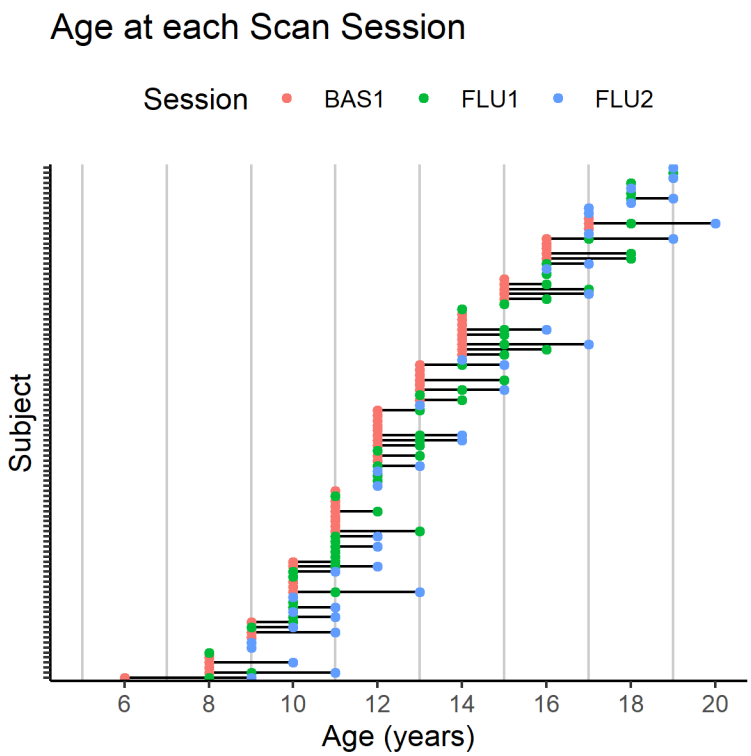

Figure 1. Age distribution at each scan session. Baseline (BAS1) sessions are denoted in red color, first follow-up (FLU1) in green, and second follow-up (FLU2) in blue. The black horizontal lines connecting the dots represent a single subject who completed multiple scan sessions.

2.2. Imaging Parameters

For the current study, we were interested in fMRI data obtained during the breath-holding task. All MRI scans were obtained using a 3.0T Siemens TIM Trio at the Nathan Kline Institute, in which a 32-channel head coil was used. The acquisition time for the T1-weighted image was 4 minutes and 18s, with 176 slices, a TR of 1900ms and TE of 2.52ms. The acquisition time for the breath-holding task was 4 minutes and 30 seconds, with 64 slices, 2x2x2 mm resolution, a TR of 1400ms, and TE of 30ms (Tobe et al., 2022).

2.3. Preprocessing

The following preprocessing steps were applied to the data: segmentation, skull-removal, realignment, framewise displacement, coregistration, normalization, and smoothing. The data were preprocessed using Statistical Parametric Mapping (SPM12) (Ashburner et al., 2014) in MATLAB version 2021a (Mathworks, Natick, MA). First, each participants' anatomical MRI image was segmented into gray matter, white matter, and cerebrospinal fluid. Each participants' functional images were realigned to the mean functional image. For all participants, the framewise displacement values of translation and rotation were calculated to determine which participants had excessive head-motion. Any participants with a mean translation or mean rotation of greater than 0.3 mm were excluded from the study. Similarly, any participant with a maximum translation or maximum rotation greater than 2 mm was excluded from the study (Figure 2). These thresholds were defined by visualizing the framewise displacement values for all subjects, while taking into consideration the fMRI isotropic voxel size of 2 mm. After eliminating participants' data due to head-motion and those with an insufficient number of timepoints, we were left with 60 participants for the BAS1 session, 55 participants for the FLU1 session, and 40 participants for the FLU2 session. Each subject's realigned functional images were coregistered to their skull-stripped anatomical image. Subsequently, normalization was performed using SPM12's diffeomorphic anatomic registration through an exponentiated lie algebra algorithm (DARTEL) (Ashburner, 2007). A study-specific template for DARTEL was first generated using each subject's segmented anatomical images. Then, DARTEL normalization was performed to warp each subject's coregistered functional images to the study-

specific template. Smoothing was also performed using a Gaussian kernel with a full-width-half-maximum (FWHM) of 6 x 6 x 6 mm^3.

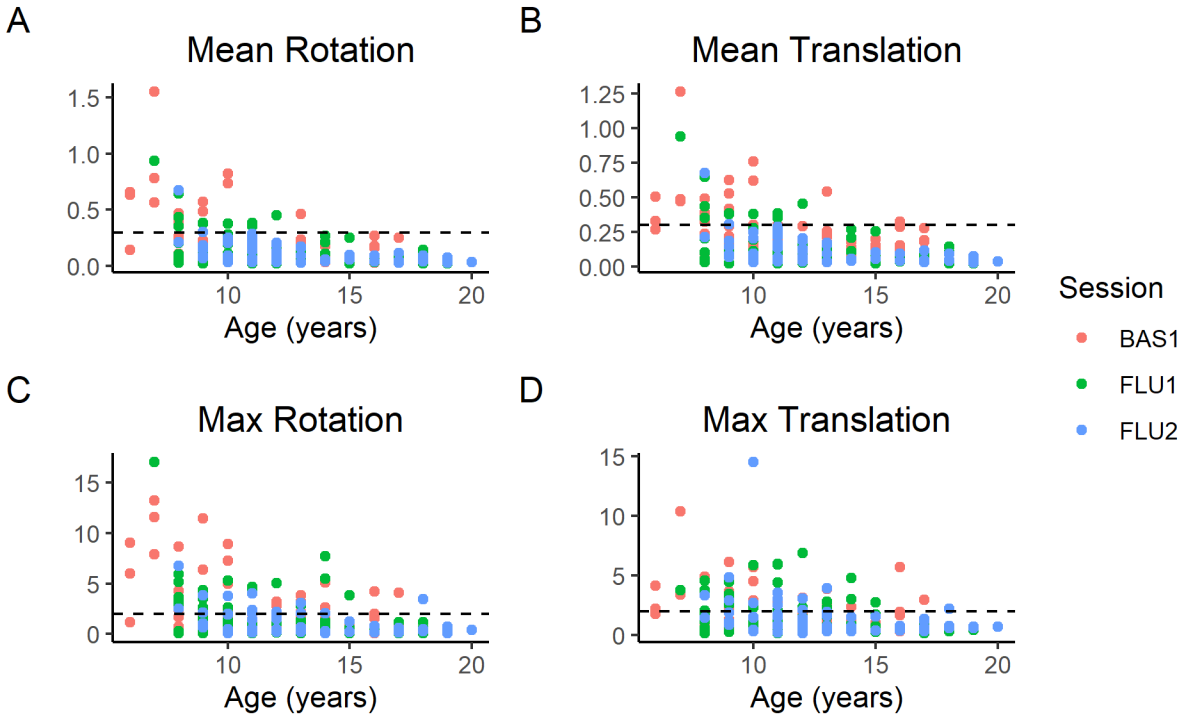

Figure 2. Framewise displacement values calculated for all participants for each age. The following framewise displacement values were calculated: A) mean rotation, B) mean translation, C) max rotation, and D) max translation. For mean values, a cut-off of 0.3 mm was chosen whereas for maximum values, a cut-off of 2 mm was chosen, as shown by the dashed lines. From the cut-off, a total of 30 subjects were excluded from the BAS1 session, 27 from the FLU1 session, and 20 from the FLU2 session.

2.4. Independent Component Analysis

Independent component analysis (ICA) was performed on a group-level for all breath-holding sessions together and then back-reconstructed on a subject-level to obtain subject-level ICA network maps. This was performed using the Group ICA of fMRI Toolbox (GIFT) (Rachakonda et al., 2007). Using the GIFT toolbox, the Infomax algorithm was used with default parameters applied, and the images were then z-scored with a threshold applied at z = 1.96. We obtained 25 independent components, and 12 of the 25 components were identified as meaningful brain networks rather than noise, thus were kept for further analyses. By using ICA, we were able to obtain spatially distinct functional brain networks, and thus reduced the number of brain areas of interest. A network-level approach rather than a voxel-wise approach allows us to reduce the dimensionality of the data and reduce issues with multiple testing.

2.5. Principal Component Analysis

To obtain a neurovascular activation measure of the breath-hold response, a principal component analysis (PCA) approach was applied to the back projected ICA mean time-series data from all subjects. PCA was performed in MATLAB v2021a. Prior to PCA, the data were standardized into z-scores. Since the first principal component explained most of the data, we focused on the first principal component for further analyses. This principal component was inferred to represent the breath-hold task activation. We decided to perform PCA instead of a general linear model, since the PCA method does not assume a particular hemodynamic response function shape or delay. This allows us to forgo any *a priori* assumptions of the hemodynamic response function (Di and Biswal, 2022; Hejnar et al., 2007).

2.6. Mixed Effects Model

Developmental effects of breath-holding activity were analyzed using a mixed-effects modeling approach. In our mixed effects model, the "age" variable was treated as a fixed effect, while the "subject" variable was assigned as a random effect. Mixed effects models are robust at handling missing data points (Yu et al., 2022). We used a mixed effects model with different assumed relationships: linear, quadratic, log, and quadratic-log to describe different developmental trajectories. These trajectories have been previously reported in developmental studies (Herting et al., 2018). We implemented the 'lme4' package in R, and transformed the 'age' variable for quadratic, log, and quadratic-log functions (Bates et al., 2015). Since the longitudinal cohort only has three timepoints, a random-intercept-only mixed effects model was used. Generally, a random slope and intercept model would require at least four timepoints to be reliable, particularly for higher-order models (King et al., 2018). The mixed effects models were formatted as follows:

Linear: PC1 Loading ~ Age + (1|subject)

Quadratic: PC1 Loading ~ Age^2 + Age + (1|subject)

Logarithmic: PC1 Loading ~ log(Age) + (1|subject)

Quadratic-log: PC1 Loading ~ $log(Age)^2$ + log(Age) + (1|subject)

2.7. Model Evaluation

We compared the different model types for each functional brain network. The linear, quadratic, log, and quadratic-log models were compared with each other to see which one provided the best fit, based on Akaike's Information Criterion (AIC) score. The AIC score was calculated based on

a maximum likelihood algorithm. We chose the AIC score as an evaluation of the goodness-of-fit of the models since no test-dataset was used and the models were all trained on the same data. The best-fitting model was chosen as the one with the lowest AIC score, which corresponds to a lower level of information loss (Portet, 2020).

2.8. Sex Effects

For each functional brain network, sex effects were evaluated by adding sex as a covariate in the mixed effects models for each brain network and each type of model: linear, quadratic, logarithmic, and quadratic logarithmic. The interaction between sex and age were also included in the mixed effects models to test for any interaction effects. T-tests using Satterthwaite's method were used to evaluate the significance of the mixed effects model terms ('lmerModLmerTest' in R) (Kuznetsova et al., 2017).

3. Results

Using ICA, the breath-hold data were decomposed into 12 identifiable functional brain networks for further analyses. All 12 IC networks are displayed using a "winner-takes-all" approach and the images were threshold at a z-score greater than 3. The following networks were defined: anterior and posterior default mode network, auditory, cingulo-opercular, frontal pole, lateral visual, left and right frontoparietal, medial visual, salience, sensorimotor, and somatosensory networks (Figure 3).

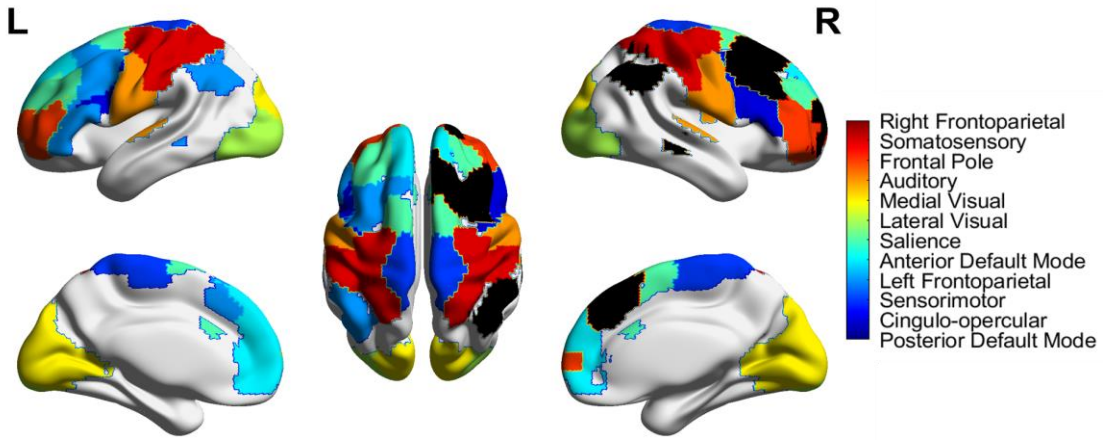

Figure 3. Map of all brain networks, visualized using BrainNetViewer (Xia et al., 2013). The IC maps are threshold at a z-score greater than 3 and displayed via a "winner-takes-all" approach.

3.1. PC1 Loading and Age

When accounting for all timepoints of data (BAS1, FLU1, FLU2), there was a positive linear trend of PC1 loading with age in the frontal pole, lateral visual, and medial visual areas, while within-individual patterns varied across networks (Figure 4). Significant age effects across different models were observed in the frontal pole, lateral visual, and medial visual areas (Table 1). The frontal pole network showed significant linear ($p = 0.0256$, 95% CI [0.0006208, 0.009775]) and log ($p = 0.0252$, 95% CI [0.008204, 0.1254]) effects of PC1 loading on age and no significant quadratic or quadratic-log effects. Similar patterns were found in the lateral and medial visual networks, displaying both significant linear and log effects of age, but weak quadratic and quadratic-log effects. The lateral visual network showed significant linear ($p = 0.0193$, 95% CI [0.0003882, 0.007092]) and log ($p = 0.0261$, 95% CI [0.002939, 0.08845]) effects of age. Although the medial visual network showed significant linear ($p = 0.0461$, 96%

CI [-7.97e-05, 0.004828]) and log (p = 0.0459, 95% CI [-0.0008697, 0.0618]) effects, the effects are weaker in comparison to the lateral visual network, since the confidence interval crosses zero. Overall, the frontal pole network had the strongest effect for log(age) relationship with a fixed effect estimate of 0.06702 (Table 1). In these three networks, there is a general increase in breath-hold activation with time; however, there is no stability within individuals, as seen from the large variability between sessions within individuals (Figure 4) (Crone and Elzinga, 2015).

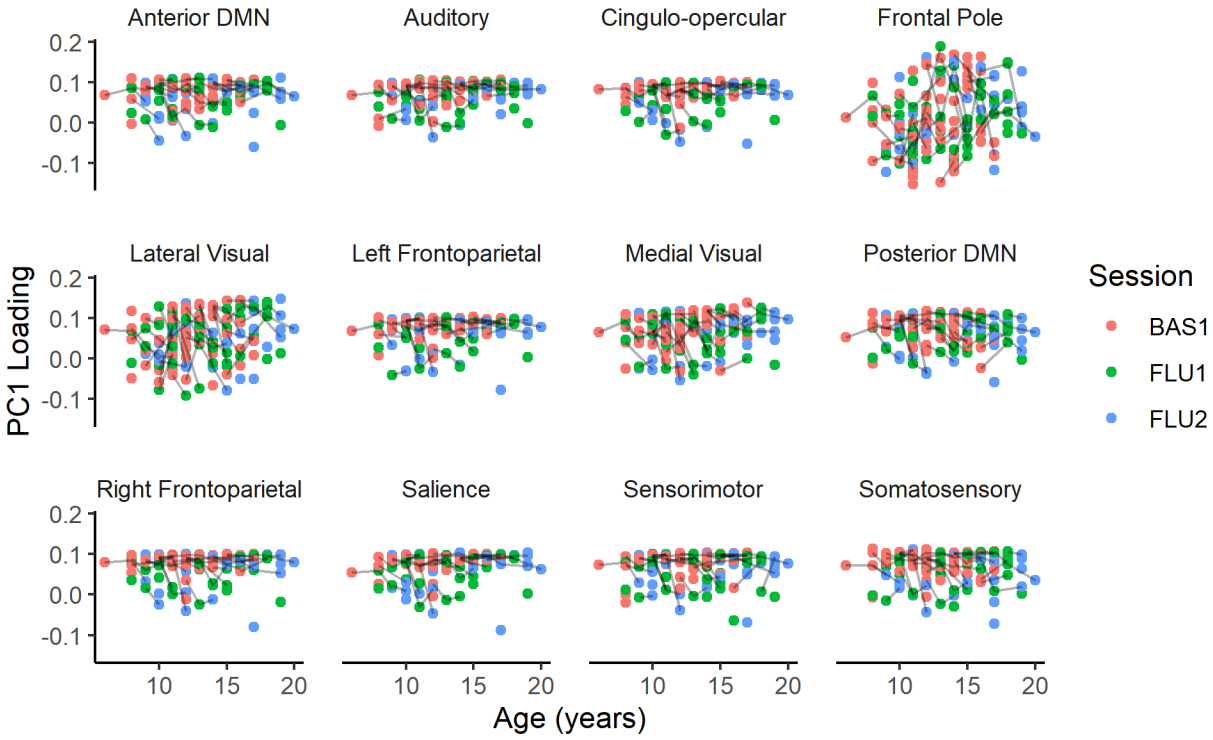

Figure 4. Relationship between PC1 loading and age for each brain network. The gray lines connecting the points represent a single subject's data, connecting from one session to another. The age ranged from 6 to 20 years of age and not all subjects completed all three sessions. Some subjects only had one timepoint of scan, shown by a single point with no connecting lines. BAS1 = baseline (red), FLU1 = first follow-up (green), and FLU2 = second follow-up scan (blue).

3.2. Model Evaluation

Based on Akaike's Information Criterion (AIC) scores, different mixed effects models provided better fits for different brain networks (Figure 5). The model which provided the lowest AIC score was considered to be the "best-fitting" model (Table S1). Overall, the logarithmic model appeared most frequently as the "best-fit" model, for the following networks: auditory, cingulo-opercular, frontal pole, right and left frontoparietal, medial visual, and salience. The linear model provided the best fit for the anterior and posterior default mode, lateral visual, sensorimotor, and somatosensory networks. The quadratic and quadratic-log models did not appear as the "best-fit" model in any of the brain networks. Focusing on the three brain networks with significant age effects, we compared the models to see which fit the best. There were no significant differences between the different models, since all AIC score differences were no larger than two units, signifying that the differences between models are minimal (Table 1) (Burnham and Anderson, 2004).

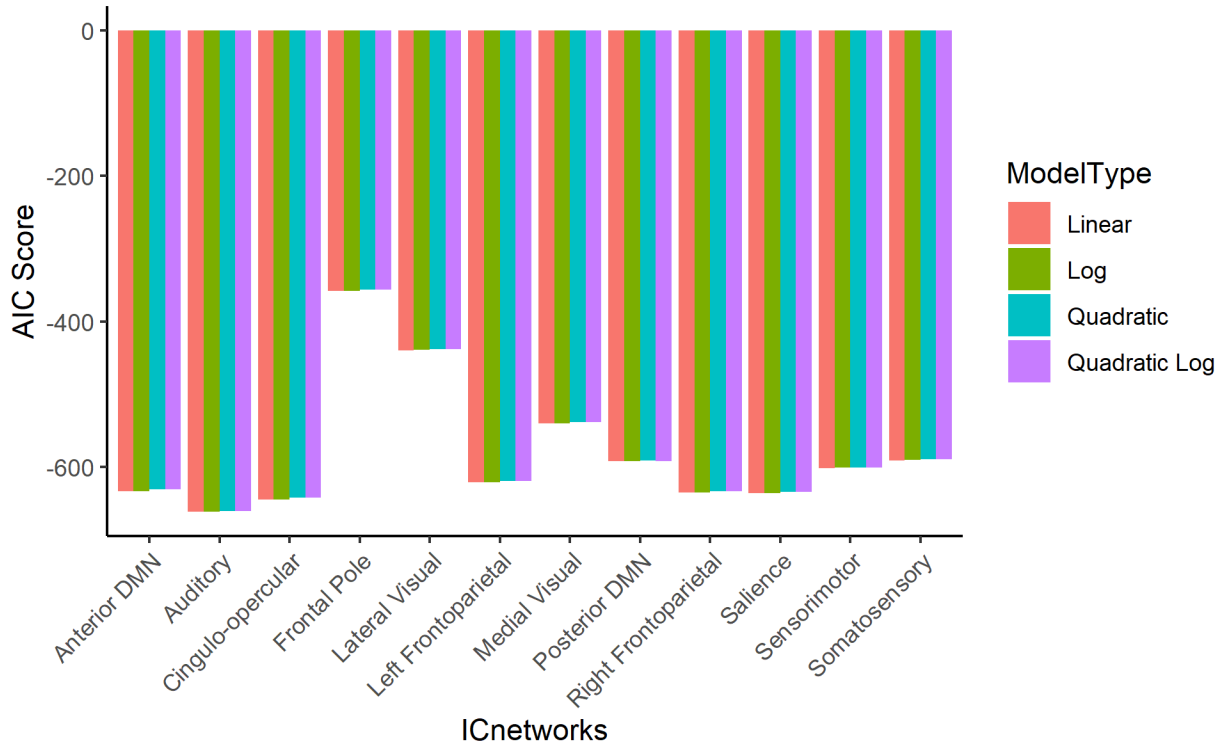

Figure 5. Mixed effects model evaluation for each brain network. Estimates were obtained using the maximum likelihood algorithm. The AIC scores for each IC brain network, and each model type: linear, log, quadratic, and quadratic-log are shown. A lower AIC score (more negative in this case) represents a better goodness-of-fit for the model. Overall, the frontal pole, lateral visual, and medial visual networks displayed the lowest AIC scores.

Table 1. Mixed effects model evaluation for functional brain networks showing significant age effects. Estimates were obtained using the maximum likelihood algorithm.

Brain Network	Model Type	Fixed Effect Estimate (Age, Age^2, log(Age), log(Age)^2)	95% Confidence Interval (Lower Bound, Upper Bound)	AIC Score	Random Effect Standard Deviation (Subject)	p-value
	Linear	0.0052190	0.0006208, 0.009775	-358.0572	0.05226	0.0256*

Frontal Pole	Quadratic	-0.0004028	-0.001676, 0.0008709	-356.4456	0.05243	0.5330
	Log	0.0670200	0.008204, 0.1254	-358.0963	0.05241	0.0252*
	Quadratic-Log	0.0274000	-0.1525, 0.2077	-356.1863	0.05223	0.7640
Lateral Visual	Linear	0.003824	0.0003882, 0.007092	-439.7202	0.01796	0.0193*
	Quadratic	0.000159	-0.0008024, 0.001107	-437.8279	0.01725	0.7400
	Log	0.046710	0.002939, 0.08845	-439.3550	0.01912	0.0261*
	Quadratic-Log	0.055120	-0.08416, 0.1923	-437.9674	0.01685	0.4230
Medial Visual	Linear	0.002417	-7.97e-05, 0.004828	-540.5658	0.01896	0.0461*
	Quadratic	-0.000119	-0.0008165, 0.0005762	-538.6795	0.01906	0.7360
	Log	0.031000	-0.0008697, 0.0618	-540.5992	0.01908	0.0459*
	Quadratic-Log	0.008017	-0.09212, 0.1078	-538.6242	0.01898	0.8740

3.3. Sex differences

We found no significant effects of sex on the PC1 loading for each mixed effects model, and no interaction effects between sex and age. For all brain networks, there were no significant effects of sex found. For the three networks that displayed significant effects of age on PC1 loading, the trajectories between males and females were similar (Figure 6).

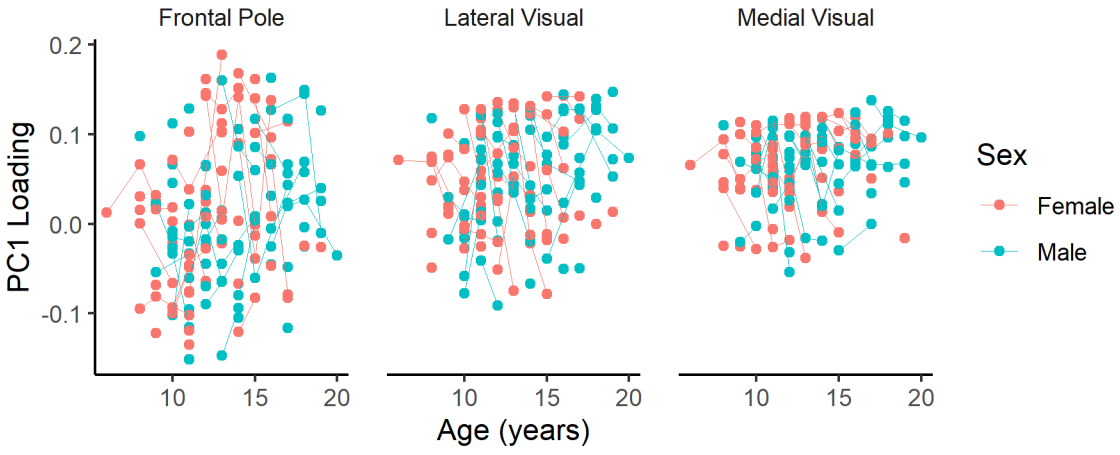

Figure 6. PC1 loading values plotted across age for the three brain networks of interest, with trajectories for females and males shown separately. The lines connecting the points resemble a single subject at different sessions.

4. Discussion

In the current study, we fit linear, logarithmic, quadratic, and quadratic-logarithmic mixed effects models to longitudinal breath-hold activation data across age, from 6 to 20 years. We found that different functional brain networks exhibited different breath-hold response trajectories across age, with linear and logarithmic models providing the best fit. In particular, the frontal pole, medial visual, and lateral visual networks displayed significant effects of breath-hold response across age. We report no sex-effects on the breath-hold response across age.

4.1. Increased activation in the frontal and visual networks

Different functional brain networks have been shown to mature at different rates across age (Gaillard et al., 2001; Zuo et al., 2010). We observed an increase in the breath-hold activation in the frontal and visual networks across age; however, we expected all regions of the brain to respond similarly across age from the breath-hold stimulus. The breath-hold response is a global response, so it influences all regions of the brain. However, it appears that across development, there are certain areas of the brain that are more susceptible to the breath-hold response or have different patterns of response.

The visual cortex showed both linear and log trends across age. Both medial and lateral visual networks showed significant positive effects of age on breath-hold activation. Marcar and

colleagues found that the BOLD response in younger children is more strongly influenced by cerebral metabolic rate of oxygen (CMRO2) and suggest that the visual system in young children is immature, thus less energy efficient than a mature visual system (Marcar et al., 2004). As age increases, the breath-hold activation was seen to increase as well, possibly indicative of the development of a more mature visual system. In animal studies, visual enrichment has been shown to increase the density of vessels per neuron (Argandoña et al., 2012). As children age, the visual system is exposed to more stimuli and thus the vasculature in the visual networks can be expected to increase. Increased vascular density in these areas may be the cause for increased breath-hold activation across age. Since the breath-hold task causes vasodilation, a denser vascular architecture may lead to increased breath-hold activation. Increased vascular maturation in the visual cortex would also lead to increased local cerebral blood flow (CBF) and cerebral blood volume (CBV), which both contribute to cerebrovascular reactivity (Bouma and Muizelaar, 1992).

Similar to the visual networks, the frontal pole network showed increased breath-hold activation across age. The frontal pole network is associated with higher-order cognitive areas and tend to mature later in life, particularly since this region is mediated by experience. The primary sensory and motor areas of the brain complete development first, whereas the association areas are the last to mature (Gaillard et al., 2001). In a longitudinal fMRI study, Ordaz and colleagues reported that motor-related regions showed no age-related changes, while error-related activity increased into early adulthood in the anterior cingulate cortex (Ordaz et al., 2013; Telzer et al., 2018). This is consistent with our findings, in which the motor-related networks showed no significant age-related changes in neurovascular reactivity. The frontal pole and visual networks are both part of the association cortex, which receive inputs from multiple

areas of the brain. It is not yet clear why the frontal pole and medial and lateral visual networks showed age-effects in neurovascular reactivity; however, it is possible that since these regions mature the latest, the vascular properties also continue to mature. We found that neurovascular reactivity is altered across age in brain network-specific patterns, similar to how brain development has been shown to be network-specific.

The frontal pole and visual networks both showed state-like variability within individuals. The other networks showed variability within individuals as well; however, there were no age-related increases in breath-hold activation across individuals. Cross-sectional fMRI studies on development may not be reflective of development, particularly when there are intra-individual variabilities that can only be studied with longitudinal data (Crone and Elzinga, 2015). The data used in the present study is longitudinal in design; however, there are only 3 separate scan sessions and not all subjects completed all scan sessions due to the challenge of subject attrition. Many fMRI studies investigating the developing brain are cross-sectional in design and this limits our understanding of development, as each child's brain is unique and may follow different trajectories of development. A cross-sectional design may overlook these unique developmental trajectories. Despite the advantages of longitudinal developmental study designs, there are challenges which limit its wide-spread usage. It is not only difficult to have participants commit to follow-up scans, but these study designs may also be very costly. Another challenge arises during the consideration of a specific task to study developmental cognitive functions. When a participant is presented with a cognitive or behavioral task, they typically respond the strongest during the initial exposure to the task. As the task is repeated multiple times, the participant may become accustomed to the task or have expectations ready, which may yield weaker responses. This is important to consider when designing longitudinal studies, since any

effects observed could simply be due to habituation. However, this does not apply to the breath-hold task since it induces hypercapnia and there are minimal habituation effects associated with hypercapnia. In addition to task-based fMRI studies, resting-state studies are also widely used in longitudinal designs, in which the participant is not asked to perform any specific task, but rather lay in the fMRI scanner in an awake and rested state. This type of design measures brain activity more intrinsically without any external stimuli, and in a longitudinal resting-state design, researchers do not have to worry about any habituation or learning effects. Yet despite the advantages of resting-state fMRI longitudinal studies, limitations also arise in terms of interpretability of the ongoing neuronal vs. vascular contributions to the blood-oxygen-level-dependent (BOLD) signal, which is yet unclear.

4.2. Trends that best describe the neurovascular response across children

We observed both linear and logarithmic trajectories of breath-hold activation across age in the frontal pole and visual networks. Although there are no longitudinal breath-hold fMRI studies that we are aware of, there have been studies investigating longitudinal developmental trajectories using cognitive task-based fMRI across children. Ordaz and colleagues longitudinally investigated the performance of an inhibitory anti-saccade task in participants aged 9 to 26 years old and observed linear effects of age in activation in the supplementary eye fields, left posterior parietal cortex, and putamen areas (Ordaz et al., 2013). Braams and colleagues investigated longitudinal changes across development in the nucleus accumbens, a region of the brain associated with rewards and risk taking and found a quadratic age pattern where a peak response to rewards was found in adolescence (Braams et al., 2015). These studies fitted linear and quadratic models to longitudinal fMRI data and chose the model which provided

the best fit to describe development. Across the different brain networks, different models to describe the developmental trajectory were fitted, which shows that the neurovascular response across age develops differentially in different brain networks and tasks. These studies used task-based fMRI and did not include breath-hold paradigms; however, the breath-hold response has been suggested to contribute to the fMRI BOLD signal activity. Therefore, the trajectories stated in previous papers could also be due in part to underlying differences in neurovascular reactivity.

Using a breath-hold paradigm, Thomason and colleagues reported significant differences between children (7-12 yrs) and adults (18-29 yrs) in the number of voxels activated across brain regions and between brain regions (Thomason et al., 2005). This showed heterogeneity in the vascular responsiveness across the brain, which was consistent with our findings of increased breath-hold activation in specific networks: the frontal pole, medial, and lateral visual networks. Regional differences in the responsiveness of the brain to the breath-hold stimulus has been shown previously by Kastrup and colleagues (Kastrup et al., 1999a); however, Thomason and colleagues were the first to test the regional effect of breath-holding between two different age groups – children and adults. We observed network-specific age effects of the breath-hold response in children enrolled in a longitudinal study.

Comparing models using the AIC score showed that there were no significant differences between the linear, quadratic, logarithmic, and quadratic-logarithmic curves. An AIC score difference of more than two units between two models indicates that one model performs significantly better than the other; however, this was not observed in our study (Portet, 2020).

4.3. No sex effects on the neurovascular response across children

For each brain network, no significant effect of sex on breath-hold activation was found. In a longitudinal fMRI study of participants aged 9 to 26 years, there were sex-effects predominantly in the motor areas of the brain as well as the executive control region in the right ventrolateral prefrontal cortex (Ordaz et al., 2013). In contrast, we found no effect of sex on the breath-hold response in the motor and executive function areas of the brain for each model fit. In a diffusion tensor imaging (DTI) study investigating structural connectivity differences between males and females across development, females were observed to have interhemispheric connectivity dominance mainly in the frontal lobe during adolescence (defined as ages 13.4-17 years), whereas during adulthood (17.1-22 years), the interhemispheric connectivity dispersed to other lobes (Ingalhalikar et al., 2014).

4.4. Limitations

One limitation of the study is the lack of subjects for the younger age range. The younger aged group (<8 years) typically has higher levels of head motion. Since we don't have measures of vascular activity for those younger than 6 years of age, it is possible that there was a logarithmic trend in many networks, but due to stabilization already occurring at 6 years of age, we cannot observe those logarithmic effects. Future studies may want to focus on more high-quality data in the younger-aged group to be more representative of development. Measures of subject compliance were also not provided for all subjects, and the measurements were very noisy, so it is not completely clear if the subjects performed the breath-hold task correctly. Younger subjects may be less compliant with the breath-hold task; however, it is understood that

parents would generally prefer having their children perform a breath-hold task than to have acetazolamide injection or varied levels of CO2 inhalation.

5. Conclusion

The current study investigated the longitudinal brain trajectories of development in children performing a breath-hold task, using fMRI. We observed that the breath-hold activation response across development follows a logarithmic trajectory overall; however, different functional brain networks may be explained better by different mixed models. We also report no sex-effects in the breath-hold response across brain networks and models.

CRediT authorship contribution statement

Donna Y. Chen: conceptualization, formal analysis, writing. **Xin Di:** conceptualization, supervision, writing - review&editing. **Bharat Biswal:** conceptualization, supervision, funding acquisition, writing - review&editing.

Declaration of competing interests

The authors declare no conflict of interest.

Acknowledgements

Research reported in this publication was supported by the National Institutes of Health (NIH) under Award Number R01MH012577 and RF1NS124778 to B.B., and R15MH125332 to X.D, and by the National Center for Advancing Translational Sciences (NCATS) of the NIH under

Award Number TL1TR003019 to D.Y.C. The content is solely the responsibility of the authors and does not necessarily represent the official views of the National Institutes of Health.

References

Abdelkarim, D., Zhao, Y., Turner, M.P., Sivakolundu, D.K., Lu, H., Rypma, B., 2019. A neural-vascular complex of age-related changes in the human brain: Anatomy, physiology, and implications for neurocognitive aging. Neurosci Biobehav Rev 107, 927-944.

Argandoña, E.G., Bengoetxea, H., Ortuzar, N., Bulnes, S., Rico-Barrio, I., Lafuente, J.V., 2012. Experience Mediated Development of the Visual Cortex Vascularization. Visual Cortex-Current Status and Perspectives. IntechOpen.

Arichi, T., Fagiolo, G., Varela, M., Melendez-Calderon, A., Allievi, A., Merchant, N., Tusor, N., Counsell, S.J., Burdet, E., Beckmann, C.F., Edwards, A.D., 2012. Development of BOLD signal hemodynamic responses in the human brain. Neuroimage 63, 663-673.

Ashburner, J., 2007. A fast diffeomorphic image registration algorithm. Neuroimage 38, 95-113.

Ashburner, J., Barnes, G., Chen, C.-C., Daunizeau, J., Flandin, G., Friston, K., Kiebel, S., Kilner, J., Litvak, V., Moran, R., 2014. SPM12 manual. Wellcome Trust Centre for Neuroimaging, London, UK 2464.

Bates, D., Mächler, M., Bolker, B., Walker, S., 2015. Fitting Linear Mixed-Effects Models Using lme4. Journal of Statistical Software 67, 1 - 48.

Bell, C.C., 1994. DSM-IV: Diagnostic and Statistical Manual of Mental Disorders. JAMA 272, 828-829.

Bouma, G.J., Muizelaar, J.P., 1992. Cerebral blood flow, cerebral blood volume, and cerebrovascular reactivity after severe head injury. J Neurotrauma 9 Suppl 1, S333-348.

Braams, B.R., van Duijvenvoorde, A.C., Peper, J.S., Crone, E.A., 2015. Longitudinal changes in adolescent risk-taking: a comprehensive study of neural responses to rewards, pubertal development, and risk-taking behavior. J Neurosci 35, 7226-7238.

Bright, M.G., Bulte, D.P., Jezzard, P., Duyn, J.H., 2009. Characterization of regional heterogeneity in cerebrovascular reactivity dynamics using novel hypocapnia task and BOLD fMRI. Neuroimage 48, 166-175.

Bright, M.G., Donahue, M.J., Duyn, J.H., Jezzard, P., Bulte, D.P., 2011. The effect of basal vasodilation on hypercapnic and hypocapnic reactivity measured using magnetic resonance imaging. J Cereb Blood Flow Metab 31, 426-438.

Bruhn, H., Kleinschmidt, A., Boecker, H., Merboldt, K.D., Hanicke, W., Frahm, J., 1994. The effect of acetazolamide on regional cerebral blood oxygenation at rest and under stimulation as assessed by MRI. J Cereb Blood Flow Metab 14, 742-748.

Burnham, K.P., Anderson, D.R., 2004. Multimodel Inference:Understanding AIC and BIC in Model Selection. Sociological Methods & Research 33, 261-304.

Church, J.A., Petersen, S.E., Schlaggar, B.L., 2010. The "Task B problem" and other considerations in developmental functional neuroimaging. Hum Brain Mapp 31, 852-862.

Crone, E.A., Elzinga, B.M., 2015. Changing brains: how longitudinal functional magnetic resonance imaging studies can inform us about cognitive and social-affective growth trajectories. Wiley Interdiscip Rev Cogn Sci 6, 53-63.

Davidson, M.C., Thomas, K.M., Casey, B.J., 2003. Imaging the developing brain with fMRI. Ment Retard Dev Disabil Res Rev 9, 161-167.

Di, X., Biswal, B.B., 2022. Principal component analysis reveals multiple consistent responses to naturalistic stimuli in children and adults. Hum Brain Mapp 43, 3332-3345.

Fair, D.A., Cohen, A.L., Power, J.D., Dosenbach, N.U., Church, J.A., Miezin, F.M., Schlaggar, B.L., Petersen, S.E., 2009. Functional brain networks develop from a "local to distributed" organization. PLoS Comput Biol 5, e1000381.

Gaillard, W.D., Grandin, C.B., Xu, B., 2001. Developmental aspects of pediatric fMRI: considerations for image acquisition, analysis, and interpretation. Neuroimage 13, 239-249.

Galiano, A., Mengual, E., Garcia de Eulate, R., Galdeano, I., Vidorreta, M., Recio, M., Riverol, M., Zubieta, J.L., Fernandez-Seara, M.A., 2020. Coupling of cerebral blood flow and functional connectivity is decreased in healthy aging. Brain Imaging Behav 14, 436-450.

Hejnar, M.P., Kiehl, K.A., Calhoun, V.D., 2007. Interparticipant correlations: a model free FMRI analysis technique. Hum Brain Mapp 28, 860-867.

Herting, M.M., Gautam, P., Chen, Z., Mezher, A., Vetter, N.C., 2018. Test-retest reliability of longitudinal task-based fMRI: Implications for developmental studies. Dev Cogn Neurosci 33, 17-26.

Iadecola, C., 2017. The Neurovascular Unit Coming of Age: A Journey through Neurovascular Coupling in Health and Disease. Neuron 96, 17-42.

Ingalhalikar, M., Smith, A., Parker, D., Satterthwaite, T.D., Elliott, M.A., Ruparel, K., Hakonarson, H., Gur, R.E., Gur, R.C., Verma, R., 2014. Sex differences in the structural connectome of the human brain. Proc Natl Acad Sci U S A 111, 823-828.

Jacobs, J., Hawco, C., Kobayashi, E., Boor, R., LeVan, P., Stephani, U., Siniatchkin, M., Gotman, J., 2008. Variability of the hemodynamic response as a function of age and frequency of epileptic discharge in children with epilepsy. Neuroimage 40, 601-614.

Kannurpatti, S.S., Motes, M.A., Biswal, B.B., Rypma, B., 2014. Assessment of unconstrained cerebrovascular reactivity marker for large age-range FMRI studies. PLoS One 9, e88751.

Kastrup, A., Kruger, G., Glover, G.H., Neumann-Haefelin, T., Moseley, M.E., 1999a. Regional variability of cerebral blood oxygenation response to hypercapnia. Neuroimage 10, 675-681.

Kastrup, A., Li, T.Q., Glover, G.H., Moseley, M.E., 1999b. Cerebral blood flow-related signal changes during breath-holding. AJNR Am J Neuroradiol 20, 1233-1238.

Kety, S.S., Schmidt, C.F., 1948. The Effects of Altered Arterial Tensions of Carbon Dioxide and Oxygen on Cerebral Blood Flow and Cerebral Oxygen Consumption of Normal Young Men. J Clin Invest 27, 484-492.

King, K.M., Littlefield, A.K., McCabe, C.J., Mills, K.L., Flournoy, J., Chassin, L., 2018. Longitudinal modeling in developmental neuroimaging research: Common challenges, and solutions from developmental psychology. Dev Cogn Neurosci 33, 54-72.

Kuznetsova, A., Brockhoff, P.B., Christensen, R.H.B., 2017. lmerTest Package: Tests in Linear Mixed Effects Models. Journal of Statistical Software 82, 1 - 26.

Kwong, K.K., Wanke, I., Donahue, K.M., Davis, T.L., Rosen, B.R., 1995. EPI imaging of global increase of brain MR signal with breath-hold preceded by breathing O2. Magn Reson Med 33, 448-452.

Luna, B., Padmanabhan, A., O'Hearn, K., 2010. What has fMRI told us about the development of cognitive control through adolescence? Brain Cogn 72, 101-113.

Marcar, V.L., Strassle, A.E., Loenneker, T., Schwarz, U., Martin, E., 2004. The influence of cortical maturation on the BOLD response: an fMRI study of visual cortex in children. Pediatr Res 56, 967-974.

Mukherjee, B., Preece, M., Houston, G.C., Papadakis, N.G., Carpenter, T.A., Hall, L.D., Huang, C.L., 2005. Mapping of the cerebral response to acetazolamide using graded asymmetric spin echo EPI. Magn Reson Imaging 23, 907-920.

Ordaz, S.J., Foran, W., Velanova, K., Luna, B., 2013. Longitudinal growth curves of brain function underlying inhibitory control through adolescence. J Neurosci 33, 18109-18124.

Portet, S., 2020. A primer on model selection using the Akaike Information Criterion. Infect Dis Model 5, 111-128.

Rachakonda, S., Egolf, E., Correa, N., Calhoun, V., 2007. Group ICA of fMRI toolbox (GIFT) manual. Dostupnez [cit 2011-11-5].

Schmithorst, V.J., Vannest, J., Lee, G., Hernandez-Garcia, L., Plante, E., Rajagopal, A., Holland, S.K., Consortium, C.A., 2015. Evidence that neurovascular coupling underlying the BOLD effect increases with age during childhood. Hum Brain Mapp 36, 1-15.

Somerville, L.H., Jones, R.M., Casey, B.J., 2010. A time of change: behavioral and neural correlates of adolescent sensitivity to appetitive and aversive environmental cues. Brain Cogn 72, 124-133.

Stillman, A.E., Hu, X., Jerosch-Herold, M., 1995. Functional MRI of brain during breath holding at 4 T. Magn Reson Imaging 13, 893-897.

Telzer, E.H., McCormick, E.M., Peters, S., Cosme, D., Pfeifer, J.H., van Duijvenvoorde, A.C.K., 2018. Methodological considerations for developmental longitudinal fMRI research. Dev Cogn Neurosci 33, 149-160.

Thomason, M.E., Burrows, B.E., Gabrieli, J.D., Glover, G.H., 2005. Breath holding reveals differences in fMRI BOLD signal in children and adults. Neuroimage 25, 824-837.

Tobe, R.H., MacKay-Brandt, A., Lim, R., Kramer, M., Breland, M.M., Tu, L., Tian, Y., Trautman, K.D., Hu, C., Sangoi, R., Alexander, L., Gabbay, V., Castellanos, F.X., Leventhal, B.L., Craddock, R.C., Colcombe, S.J., Franco, A.R., Milham, M.P., 2022. A longitudinal resource for studying connectome development and its psychiatric associations during childhood. Sci Data 9, 300.

Tsvetanov, K.A., Henson, R.N., Tyler, L.K., Davis, S.W., Shafto, M.A., Taylor, J.R., Williams, N., Cam, C., Rowe, J.B., 2015. The effect of ageing on fMRI: Correction for the confounding effects of vascular reactivity evaluated by joint fMRI and MEG in 335 adults. Hum Brain Mapp 36, 2248-2269.

Uddin, L.Q., Supekar, K., Menon, V., 2013. Reconceptualizing functional brain connectivity in autism from a developmental perspective. Front Hum Neurosci 7, 458.

Van Horn, J.D., Pelphrey, K.A., 2015. Neuroimaging of the developing brain. Brain Imaging Behav 9, 1-4.

West, K.L., Zuppichini, M.D., Turner, M.P., Sivakolundu, D.K., Zhao, Y., Abdelkarim, D., Spence, J.S., Rypma, B., 2019. BOLD hemodynamic response function changes significantly with healthy aging. Neuroimage 188, 198-207.

Xia, M., Wang, J., He, Y., 2013. BrainNet Viewer: a network visualization tool for human brain connectomics. PLoS One 8, e68910.

Yu, Z., Guindani, M., Grieco, S.F., Chen, L., Holmes, T.C., Xu, X., 2022. Beyond t test and ANOVA: applications of mixed-effects models for more rigorous statistical analysis in neuroscience research. Neuron 110, 21-35.

Zimmerman, B., Rypma, B., Gratton, G., Fabiani, M., 2021. Age-related changes in cerebrovascular health and their effects on neural function and cognition: A comprehensive review. Psychophysiology 58, e13796.

Zuo, X.N., Kelly, C., Di Martino, A., Mennes, M., Margulies, D.S., Bangaru, S., Grzadzinski, R., Evans, A.C., Zang, Y.F., Castellanos, F.X., Milham, M.P., 2010. Growing together and growing

apart: regional and sex differences in the lifespan developmental trajectories of functional homotopy. J Neurosci 30, 15034-15043.